HHS Public Access

Author manuscript

Pediatr Blood Cancer. Author manuscript; available in PMC 2023 November 01.

Published in final edited form as:

Pediatr Blood Cancer. 2023 November ; 70(11): e30628. doi:10.1002/pbc.30628.

Assessing the Role of Positron Emission Tomography and Bone Scintigraphy in Imaging of Pleuropulmonary Blastoma (PPB): A Report from the International PPB/*DICER1* Registry

Kelly N. Hagedorn, MD[*,1], **Alexander T. Nelson, BS**[*,2,3,4,5], **Alexander J. Towbin, MD**[6,7], **Nicole Frederickson, BA**[2,3,4], **Paige Mallinger, MS**[2,3,4], **John T. Lucas Jr, MD**[8], **Louis P. Dehner, MD**[9], **Yoav H. Messinger, MD**[2,3,4], **Barry L. Shulkin, MD**[10], **William A. Mize, MD**[1], **Kris Ann P. Schultz, MD**[2,3,4]

[1]Department of Radiology, Children's Minnesota, Minneapolis, MN;

[2]International Pleuropulmonary Blastoma/*DICER1* Registry, Children's Minnesota, Minneapolis, MN;

[3]International Ovarian and Testicular Stromal Tumor Registry, Children's Minnesota, Minneapolis, MN;

[4]Cancer and Blood Disorders, Children's Minnesota, Minneapolis, MN;

[5]University of Minnesota Medical School, Minneapolis, MN;

[6]Department of Radiology, Cincinnati Children's Hospital Medical Center, Cincinnati, OH;

[7]Department of Radiology, University of Cincinnati College of Medicine, Cincinnati, OH;

[8]Department of Radiation Oncology, St. Jude Children's Research Hospital, Memphis, TN;

[9]Lauren V. Ackerman Laboratory of Surgical Pathology, Department of Pathology and Immunology, Washington University School of Medicine, St. Louis, MO;

[10]Department of Diagnostic Imaging, St. Jude Children's Research Hospital, Memphis, TN;

Abstract

Background: Pleuropulmonary blastoma (PPB) is the most common primary lung neoplasm of infancy and early childhood. Given the rarity of PPB, the role of positron emission tomography (PET) and bone scintigraphy (bone scans) in diagnostic evaluation and surveillance has not been documented to date. Available PET and bone scan data are presented in this study.

Procedures: Patients with PPB enrolled in the International PPB/*DICER1* Registry and available PET imaging and/or bone scan reports were retrospectively abstracted.

Results: On retrospective analysis, 133 patients with type II and III (advanced) PPB were identified with available report(s) (PET scan only=34, bone scan only=83, and both bone scan

Corresponding Author: Kris Ann P. Schultz, MD, Cancer and Blood Disorders, 2530 Chicago Avenue South, Minneapolis, MN 55404, 612-813-5940, FAX: 612-813-6325, KrisAnn.Schultz@childrensmn.org.

*these authors contributed equally to this work

Conflicts of interest: The authors have no conflicts of interest to disclose.

and PET=16). All advanced primary PPB (n=11) and recurrent (n=8) tumors prior to treatment presented with ^{18}F-fluorodeoxyglucose (FDG)-avid lesions with median maximum standardized uptake values of 7.4 and 6.7, respectively. False positive FDG uptake in the thorax was noted during surveillance (specificity – 59%). Bone metastases were FDG-avid prior to treatment. Central nervous system metastases were not discernable on PET imaging. Sensitivity and specificity of bone scans for metastatic bone disease were 89% and 92%, respectively. Bone scans had a negative predictive value of 99%, although positive predictive value was 53%. Four patients with distant bone metastases had concordant true positive bone scan and PET.

Conclusion: Primary, recurrent, and/or extracranial metastatic PPB presents with an FDG-avid lesion on PET imaging. Additional prospective studies are needed to fully assess the utility of nuclear medicine imaging in surveillance for patients with advanced PPB.

Keywords

Pleuropulmonary blastoma; Type II PPB; Type III PPB; PET; Bone Scan; *DICER1* ; *DICER1*-Related Tumor Predisposition

INTRODUCTION

Pleuropulmonary blastoma (PPB) is the most common primary malignant lung neoplasm of infancy and early childhood. PPB has the potential to progress from a purely cystic lesion (type I PPB) to a high-grade primitive sarcoma with either mixed cystic and solid features (type II PPB) or to a solid lesion (type III PPB). Since type II and III PPB have a propensity to metastasize to bone[1], Technetium 99m-methylenedisphosphonate skeletal scintigraphy scan (bone scan) has been utilized as part of the staging of advanced (type II and III) PPB. In contrast, type I PPB has not been shown to present with metastatic disease and given its cystic nature[2], bone scans have not been recommended.

The International PPB (now PPB/*DICER1*) Registry (the Registry) was established in 1987 with the goal of investigating and improving outcomes for children diagnosed with this rare tumor.[3] As the Registry evolved, imaging guidelines were provided which included consideration of bone scan and/or ^{18}F-fluorodeoxyglucose (FDG) positron emission tomography (PET)/computed tomography (CT) scan, based on institutional availability, at diagnosis, week 16, week 28, and at the end of therapy for patients with type II or III PPB. Although Registry guidelines are provided, the ultimate imaging course is at the discretion of the treating institution.

PET/CT is a highly sensitive and specific imaging modality used to stage other pediatric malignancies.[4,5] In children with other types of sarcomas, PET has been shown to provide important additional information in comparison to other imaging modalities (ultrasound, CT, MRI and bone scan).[6] However, to date, data describing the role of PET/CT in PPB are limited to case reports.[7,8] Due to the fact that PPB is uncommon in relation to other malignancies in childhood, the role of PET/CT or PET/MRI and bone scan in diagnostic evaluation/staging and surveillance has not been well established or documented. The purpose of this study is to describe and compare PET and bone scintigraphy imaging observations in patients with advanced PPB from the Registry.

METHODS

Individuals of any age with suspected PPB were enrolled in the Registry. Enrollment began at the induction of the Registry in 1987 and included retrospective enrollment for patients diagnosed as early as 1973. Written informed consent and assent (when applicable) were obtained. All study procedures were approved by the Children's Minnesota institutional review board and relevant human subjects' committees (protocol #1611–130, #0909–082, #98107, ClinicalTrials.gov identifier: NCT03382158). This analysis was restricted to individuals with initial diagnoses of type II or III PPB. All imaging evaluations and treatment decisions remained at the discretion of the individual treatment teams. All imaging records relevant to PPB diagnosis and surveillance were requested from the patient's primary treating institutions and, when applicable, from additional treating institutions. Imaging records for each individual patient were retrospectively abstracted. Follow up was attempted annually.

All suspected PPBs referred to the Registry are reviewed by a Registry pathologist. In cases where central review could not distinguish between type II and type III, a diagnosis of type II/III PPB, not otherwise specified was reported and grouped with type III for this analysis. Upon central pathology confirmation, patients were included in this study if they had undergone a PET/CT, PET/MRI, and/or planar bone scan and the corresponding imaging report(s) was submitted to the Registry.

Data from the clinical imaging reports from the treating institutions were systematically extracted by Registry personnel and correlated with clinical status of the patient. All imaging reports for this study were centrally reviewed by a Registry radiologist (KNH). Findings were collated for each scan. Extracted PET data included the size, location, and corresponding maximum standardized uptake values (SUV_{max}) of all identified lesions. When data were missing, subjective descriptions were reported. For bone scans, radiotracer uptake and whether bone metastases were present on conventional imaging (X-ray, CT and/or MRI) were abstracted from radiology reports. The following general information was also included: sex, age at diagnosis, year of diagnosis, country of origin, initial PPB diagnosis and number of scans; these were collected for each participant and were evaluated using standard descriptive statistics. Clinical course and outcome were ascertained for each participant.

Sensitivity, specificity, positive predictive value (PPV), and negative predictive value (NPV) were calculated, when applicable. For PET scans to qualify for comparison, the patient could not be undergoing treatment (chemotherapy or radiation). True positive (TP), false positive (FP), true negative (TN), and false negative (FN) classification were defined for PET and bone scan (Table 1). For PET scans, when assessing the primary disease site, five clinical contexts were compared: diagnosis pre-resection, diagnosis post-resection with macroscopic residual disease, post-resection with no residual disease, surveillance, and recurrence pre-treatment. Both bone and central nervous system (CNS) metastases were assessed at both diagnosis and disease progression prior to initiation of treatment. For bone scans, each patient was classified once overall with one or more TP, FP, or FN resulting in the respective categorization regardless of whether other scans were TN. Abnormal uptake at the site of

prior thoracotomy was not considered to be a FP finding on bone scan. Classification was undertaken with careful attention to outcome data as bone metastases and recurrent disease are known to be associated with a dismal prognosis.

RESULTS

There were 605 patients with central pathology confirmation of PPB who were enrolled in the Registry; 348 of whom were diagnosed with type II or III PPB. Through retrospective review, 133 patients with type II or III PPB with either FDG PET/CT or FDG PET/MRI (referred to as PET from here forward) scan or bone scan or both were identified (Fig. 1). All included bone scans were planar and no single photon emission computed tomographic (SPECT)/CT scans were identified. All PET scans had corresponding anatomical imaging (CT or MRI). Demographic information related to participants is included in Table 2. Bone scan(s) and/or PET scan(s) were available for Registry participants who underwent treatment from 1983 to 2022. Among those included, 34 had a PET scan only, 83 had a bone scan only, and 16 had both PET and bone scan(s). When considering the number of scans per patients 52% (26/50) underwent more than one PET with a maximum of 10 and 46% (46/99) underwent more than one bone scan with a maximum of 16. Females represented 56% (75/133) of the cohort, and most participants were from the United States. Median age at diagnosis was 36 months (range: 3 – 235).

A total of 118 PET-based imaging studies (110 PET/CT and 8 PET/MRI) were performed in 50 patients. PET scans were performed at initial diagnosis or during primary treatment in 36 patients, during surveillance in 16 patients and at time of disease relapse in 16 patients. A total of 233 bone scans were performed in 99 patients. Bone scans were performed at initial diagnosis or during primary treatment in 93 patients, during surveillance in 31 patients and at relapse in 15 patients. A summary of the relative SUV_{max} values for each clinical context can be found in Table 3.

PET - Diagnosis

When considering the 36 patients with PET scans obtained at diagnosis or during primary treatment, 11 patients with type II or III PPB underwent PET scan prior to resection and chemotherapy. The remaining 25 patients had scans that were obtained following resection and/or during chemotherapy. FDG-avid lesions at the primary tumor site were reported in all 11 patients (all TP; sensitivity – 100%) (Table 3). SUV_{max} values were reported in nine patients ranging from 2 to 16.2 with a median SUV_{max} of 7.4. The other two patients had FDG-avid lesions without reported SUV_{max} values. The lesions were subjectively described; “marked FDG avidity” and “intense uptake seen within the large left chest mass”.

Of the patients with PET at diagnosis, two had subsequent PET evaluation during neoadjuvant chemotherapy. Both patients demonstrated metabolic response to chemotherapy with reduction of SUV_{max} of 77% (13 to 3) and 61% (6.4 to 2.5), respectively. The comparative size reduction, per RECIST 1.1 criteria[9], was 40% (10 to 6 cm) and 37% (5.1 to 3.2 cm), respectively.

Four patients with type II or III PPB underwent partial tumor resection and were evaluated by postoperative PET prior to initiation of chemotherapy. FDG-avid lesions at the site of residual disease were reported in all four (sensitivity - 100%) patients with median SUV_{max} of 4.6 (range: 3.3 – 7).

Postoperative PET scans were performed in six patients with upfront gross total resection and pathologically confirmed negative margins. FDG uptake at the surgical site was visible in 67% (4/6) of patients reflecting expected post-operative changes. The SUV_{max} was measured near the postoperative sites in two patients with values of 2.8 and 1.5, respectively. The reports of the two additional patients included a subjective description of mild uptake near the postoperative site. The other two patients had no reported increased FDG uptake.

PET – Recurrence/Surveillance

Eight patients were identified who had PET imaging at the time of pathologically confirmed recurrent PPB in the chest. In all eight patients (all TP; sensitivity - 100%), PET-avid lesions at the site of recurrent disease were noted with a median SUV_{max} of 6.1 (range: 1.6 – 12.7) (Table 3). Notably, recurrent disease was identified in one patient while asymptomatic. PET/MRI demonstrated FDG-avid recurrent disease in the right middle lobe with a SUV_{max} of 6. Fig. 2A represents surveillance PET findings prior to detection of recurrent disease and Fig. 2B represents the asymptomatic detection of an FDG-avid lesion. Additionally, one patient had increased FDG activity (SUV_{max} of 2) at the right hemidiaphragm and non-FDG-avid, nodular right pleural enhancement with right pleural effusion concerning for recurrent disease. Despite not undergoing surgical evaluation, the patient was treated with chemotherapy. This case was deemed indeterminate for recurrence given the lack of pathologically confirmed disease. The patient remains in remission 180 months from initial PPB diagnosis.

Overall, 27 PET scans were performed in 16 patients during surveillance after original diagnosis, resection, and treatment of type II or III PPB (13 patients) or following treatment of recurrent PPB (3 patients). Five of 16 (31%) patients had one or more scans with FP FDG uptake at or near the site of original disease (specificity – 69%) with a median SUV_{max} of 3 (range 1.3 – 5.3). The remaining 11 patients had TN PET at the time of surveillance imaging, and none had evidence of disease on conventional imaging.

PET – Identification of metastatic disease

Three patients with distant bone metastases at diagnosis underwent PET imaging prior to surgery and chemotherapy. All three patients had FDG-avid metastatic lesions (all TP; sensitivity −100%) (Table 3). The median SUV_{max} of the metastatic lesions was 2.5 (range 2 – 3.8). Bone metastases were present in two patients at the time of tumor relapse. FDG-avid metastatic lesions were identified in both patients (both TP; sensitivity - 100%) with SUV_{max} of 2.9 and 3.4, respectively. In all five patients, lesions suspicious for malignancy were noted on other imaging modalities. No false positive distant bone FDG uptake was noted.

Three patients underwent PET/CT with central nervous system metastasis. In each of these patients, there were no reported FDG-avid lesions (all FN) although 2 demonstrated

decreased uptake at the site of the lesion compared to surrounding brain parenchyma. No SUV values were available from the reports. One patient had a PET/CT that demonstrated a large metastasis in the right occipital lobe with relatively low uptake. Follow-up brain MRI demonstrated a multiloculated cystic lesion of the right occipital lobe, a small lesion in the parietal lobe, and leptomeningeal disease. Another patient had multiple enhancing lesions on MRI with no evidence of corresponding abnormal FDG uptake on subsequent PET scan. The final patient had an area of relatively decreased uptake in left parietal lobe thought to be secondary to prior surgery. MRI showed a large lesion in the parietal lobe near the site of the previous tumor bed.

Bone Scan – Identification of metastatic disease

Overall, bone scans were performed in 99 patients. Of the patients included in this analysis, nine had bone metastases, eight at initial diagnosis and one at relapse, and 90 had no bone metastases. There were seven patients with a false positive result and one false negative result. The sensitivity was 89% (8/9) and specificity was 92% (83/90) for bone scans in the evaluation for bone metastases in patients with PPB. Positive predictive value and NPV were 53% and 99%, respectively.

Nine patients had bone metastases on other imaging modalities, eight patients (1 with type II and 7 with type III PPB) at diagnosis and one patient (type III PPB) at relapse. There were eight true positive bone scans with metastatic radiotracer uptake. One patient had a false negative bone scan despite a CT showing scattered bone metastases and a biopsy confirmed diagnosis. Representative bone scan images with initial bone metastases at diagnosis prior to treatment (Fig. 3A) and subsequent response to chemotherapy (Fig. 3B) of the right femur are included.

Seven patients with at least one false positive bone scan were observed, excluding the expected chest wall findings secondary to thoracotomy site incision. One patient underwent biopsy without evidence of metastatic disease. Alternate diagnoses included bone contusion or subacute infarction, fracture, and indeterminate radiotracer uptake. None of these patients developed bone metastases. The 83 remaining patients with bone scans at diagnosis did not have any identified bone metastases (TN).

PET and bone scan

In total, 16 patients had both PET and bone scans during their disease course. Eight had both studies performed at similar time points. Four patients with metastatic disease had concordant and TP bone scan and PET (Table 3). One patient had concordant FP PET and bone scan suspicious for rib invasion. In this patient, subsequent rib resection was negative for rib invasion by PPB on pathology. Three patients had concordant TN scans.

DISCUSSION

In this analysis, we describe the use of PET imaging and bone scans in patients with PPB at diagnosis, during therapy and surveillance, and at relapse. Bone scans have been used extensively in patients with types II and III PPB with nearly 30% of participants enrolled in the Registry having at least one bone scan report available. PET has been used

less frequently (14% of patients with types II and III PPB) although many patients were diagnosed prior to PET being widely available. Half of the patients with PET scans included in this analysis were diagnosed during or after 2017. In contrast, bone scans were widely distributed with 50% of patients included diagnosed prior to 2007, although it is noted that Registry ascertainment of imaging has improved over time. These data provide insight into the role of PET in children with types II and III PPB.

Our findings are supportive of the clinical utility of PET in the evaluation of patients with types II and III PPB, although further investigation is needed. All primary and recurrent tumors were FDG-avid with a median SUV_{max} of 7.4 and 6.1, respectively. These findings provide evidence that type II and III PPB are FDG-avid prior to initiation of therapy. Two patients with PET imaging at diagnosis and after initiation of therapy demonstrated a decrease of tumoral SUV_{max} as well as a decreased size of the tumor. Further studies are needed to determine if semiquantitative analysis of PET (SUV_{max}) can predict tumor response or provide prognostic information related to the initiation of chemotherapy. While these data show promise, the overall performance of PET during surveillance was mixed. Of 16 patients who did not have confirmed recurrent disease during surveillance, five demonstrated FDG-avid lesions in the thorax, although median SUV_{max} was less (3 vs 6.1) than that of pathologically proven recurrent PPB. Further study is needed to identify features of recurrent disease during surveillance.

The use of PET imaging in surveillance requires further discussion. The relatively high FP rate of PET in these patients may lead to excess biopsy, morbidity, and cost. Although we note a specificity of 59%, it is important to note that some FP results likely reflected post-surgical changes or other findings of nonmalignant etiology, but malignancy could not be excluded. Clinical judgement is important and will influence the clinical utility of PET scans. Although post-operative inflammatory changes are expected to progressively decrease overtime, they have been shown to result in false-positive findings on PET scans in other lung malignancies up to 6 months after resection.[10] The use of radiation therapy is another consideration when assessing results during surveillance. Radiation can result in well-defined intense FDG uptake up to 6 months after treatment and hypermetabolic activity may persist up to 2 years after treatment, although at lower intensity.[11,12]

PET imaging exposes patients to radiation, and depending on their age, anesthesia may be needed. Children with type II or III PPB already undergo approximately sixteen CT scans during their treatment, raising concern for lifetime radiation exposure. It is not known if diagnostic radiation further increases the risk of subsequent cancers in patients with PPB, which is linked to germline *DICER1* variants in more than 70% of individuals,[13] however, the addition of PET imaging to CT increases the overall exposure. While PET/MRI decreases the radiation dose compared to PET/CT, this modality is not available at most pediatric centers.

Bone metastases in PPB are rare but represent an important subset of patients that face a dismal prognosis. Thus, early recognition plays an important role in therapeutic decision making. In our study, the specificity of bone scans in detecting distant bone metastases was 89%. Notably, bone metastases were confirmed on conventional imaging in all patients

including the individual with a false negative finding (pathologically confirmed). The sensitivity of PET scans for distant bone metastases was 100%, although only five patients with distant bone metastases had available imaging. Concordant results were noted in patients with both bone and PET scans with bone metastases. Bone scan demonstrated a high negative predictive value (99%) in our cohort for the detection of bone metastases, excluding disease at diagnosis and during surveillance. Although the NPV was high, the PPV was relatively low (53%) with FP bone scans distinguished from true bone metastases based on conventional imaging. The relatively low PPV of bone scans may lead to additional imaging, in contrast to PET scans not having any false positive distant bone metastases. Notably, all bone scans were planar, and SPECT/CT may improve diagnostic accuracy over planar imaging alone.[14,15] Of consideration, the use of bone scan is associated with a lower cost and radiation dose as compared to PET. Although the negative predictive value of bone scan is appealing, lower positive predictive value limits the utility of bone scan. Additionally, we suspect that small sites of disease detectable by PET imaging may not be detected by bone scan.

When available and feasible, PET may be helpful given the additional benefit of paired anatomic imaging allowing a more comprehensive staging evaluation, the ability to provide information related to local recurrence in the chest and potential for evaluation of tumor response during neoadjuvant chemotherapy. In other soft tissue sarcomas, studies have demonstrated that PET scans may be useful in prognostication and determining histopathologic response to chemotherapy.[16–19]

Our study highlights three patients with CNS metastases who underwent PET imaging but did not have corresponding relative increased tumoral FDG uptake. We hypothesize this is due to the intense background physiologic brain FDG uptake or the tumors were too small for accurate metabolic characterization by PET. Based on the description in the reports we believe that metastatic lesions have similar or decreased uptake compared to the background brain parenchyma. Because of this limitation of ^{18}F-FDG PET, brain MRI remains a critical component in the evaluation of advanced PPB at diagnosis and during treatment and during surveillance. Currently, we recommend brain MRI at diagnosis of type II or III PPB, at weeks 13 and 28 during therapy, at end of therapy, and 3 months during years 1 and 2, and at least every 6 months during year 3 following the end of therapy. Additionally, brain MRI should be completed during staging of relapsed disease and when clinical symptoms indicate possible CNS metastasis. Alternative PET radiotracers have been studied in CNS lesions and may be helpful for patients with PPB and questionable or equivocal MRI findings.[20,21]

There are several limitations of this study. Notably, this cohort of patients underwent imaging at the discretion of the local institution. The data presented here represents available, not protocol-required imaging and could thus be influenced by the diagnostic imaging preferences of the local institution. Additionally, because management of individuals in the International PPB/*DICER1* Registry remains at the discretion of the treating institution, time points of PET and bone scans varied among the patients, limiting comparison data. The treating institution reports were used for abstraction, limiting the uniformity of the data collection. The quality of imaging and reports were variable, as imaging was completed over nearly 40 years for bone scans and 20 years for PET scans.

Next, it is likely that the number of PET imaging or bone scans is undercounted as some institutions may use external sites for nuclear medicine imaging. Most individuals were from the United States leading to under representation of international patients likely because of logistical challenges of collecting imaging data from some international institutions and increased accessibility, specifically to PET, in the United States. To qualify as false positives, confirmation of negative pathology was not required due to limited available data. It is expected that pathologic confirmation would have provided a better benchmark comparison versus conventional imaging. Finally, the data may contain referral bias as patients at risk for or known to have recurrence may have been more likely to undergo longitudinal imaging.

Nonetheless, this represents the largest analysis of nuclear medicine imaging in PPB to date and provides background data to support the further evaluation of PET imaging in the staging and surveillance of children with types II and III PPB. As further data are collected, it will be important to monitor any changes in surveillance and intervention plan based on PET imaging.

In conclusion, PET was highly sensitive in patients with type II or III PPB demonstrating FDG-avid primary, recurrent, and (non-CNS) metastatic lesions. Bone metastases can be detected by both bone scan and PET and no false positive bone metastases were noted with PET imaging. Brain MRI remains the standard of care for assessing for CNS metastases. Additional prospective studies are needed to fully assess the utility of nuclear medicine imaging for patients with advanced PPB.

Acknowledgments:

The authors wish to thank the many treating physicians, genetic counselors, patients, and families who collaboratively support the International PPB/*DICER1* Registry as well as the Pine Tree Apple Classic Fund whose volunteers, tennis players and donors have provided more than 35 years of continuous support for PPB Research. The authors gratefully acknowledge the contributions of Jason Albrecht to ongoing PPB research initiatives. The International PPB/*DICER1* Registry is also supported by the Children's Minnesota Foundation, Mendon F. Schutt Foundation and Rein in Sarcoma.

This analysis was supported by a grant from the Children's Minnesota Internal Research Grant Program and supported by funding from National Institute of Health National Cancer Institute grants 1R37CA244940-01 and 2R01CA143167-06A1.

Data Availability Statement:

The data that support the findings are not publicly available due to privacy or ethical restrictions and can be requested from the corresponding author.

Glossary

Bone scan	Bone scintigraphy scans
CNS	Central nervous system
CT	Computed tomography
FDG	^{18}F-fluorodeoxyglucose
FN	False negative

FP	False positive
MRI	Magnetic resonance imaging
NPV	Negative predictive value
PET	Positron emission tomography
PPB	Pleuropulmonary blastoma
PPV	Positive predictive value
Registry	International PPB/DICER1 Registry
SPECT	Single photon emission computed tomographic
SUV_{max}	Maximum standardized uptake values
TN	True negative
TP	True positive

REFERENCES

1. Schultz KAP, Harris AK, Nelson AT, Watson D, Lucas JT Jr., Miniati D, et al. Outcomes for Children With Type II and Type III Pleuropulmonary Blastoma Following Chemotherapy: A Report From the International PPB/DICER1 Registry. J Clin Oncol. 2023;41(4):778–789. [PubMed: 36137255]
2. Nelson AT, Harris AK, Watson D, Miniati D, Finch M, Kamihara J, et al. Type I and Ir pleuropulmonary blastoma (PPB): A report from the International PPB/DICER1 Registry. Cancer. 2023;129(4):600–613. [PubMed: 36541021]
3. Manivel JC, Priest JR, Watterson J, Steiner M, Woods WG, Wick MR, et al. Pleuropulmonary blastoma. The so-called pulmonary blastoma of childhood. Cancer. 1988;62(8):1516–26. [PubMed: 3048630]
4. Uslu L, Donig J, Link M, Rosenberg J, Quon A, Daldrup-Link HE. Value of 18F-FDG PET and PET/CT for evaluation of pediatric malignancies. J Nucl Med. 2015;56(2):274–86. [PubMed: 25572088]
5. Federico SM, Spunt SL, Krasin MJ, Billup CA, Wu J, Shulkin B, et al. Comparison of PET-CT and conventional imaging in staging pediatric rhabdomyosarcoma. Pediatr Blood Cancer. 2013;60(7):1128–34. [PubMed: 23255260]
6. Völker T, Denecke T, Steffen I, Misch D, Schönberger S, Plotkin M, et al. Positron emission tomography for staging of pediatric sarcoma patients: results of a prospective multicenter trial. J Clin Oncol. 2007;25(34):5435–41. [PubMed: 18048826]
7. Ruan D, Sun L. Case Report: Pleuropulmonary Blastoma in a 2.5-Year-Old Boy: 18F-FDG PET/CT Findings. Case Report. 2021;1
8. Geiger J, Walter K, Uhl M, Bley TA, Jüttner E, Brink I, et al. Imaging findings in a 3-year-old girl with type III pleuropulmonary blastoma. In Vivo. 2007;21(6):1119–22. [PubMed: 18210767]
9. Eisenhauer EA, Therasse P, Bogaerts J, Schwartz LH, Sargent D, Ford R, et al. New response evaluation criteria in solid tumours: revised RECIST guideline (version 1.1). Eur J Cancer. 2009;45(2):228–47. [PubMed: 19097774]
10. Kanzaki R, Higashiyama M, Maeda J, Okami J, Hosoki T, Hasegawa Y, et al. Clinical value of F18-fluorodeoxyglucose positron emission tomography-computed tomography in patients with non-small cell lung cancer after potentially curative surgery: experience with 241 patients. Interact Cardiovasc Thorac Surg. 2010;10(6):1009–14. [PubMed: 20197344]

11. Hoopes DJ, Tann M, Fletcher JW, Forquer JA, Lin PF, Lo SS, et al. FDG-PET and stereotactic body radiotherapy (SBRT) for stage I non-small-cell lung cancer. Lung Cancer. 2007;56(2):229–34. [PubMed: 17353064]
12. Matsuo Y, Nakamoto Y, Nagata Y, Shibuya K, Takayama K, Norihisa Y, et al. Characterization of FDG-PET images after stereotactic body radiation therapy for lung cancer. Radiother Oncol. 2010;97(2):200–4. [PubMed: 20430463]
13. Brenneman M, Field A, Yang J, Williams G, Doros L, Rossi C, et al. Temporal order of RNase IIIb and loss-of-function mutations during development determines phenotype in pleuropulmonary blastoma / DICER1 syndrome: a unique variant of the two-hit tumor suppression model. F1000Res. 2015;4:214. [PubMed: 26925222]
14. Zhang Y, Shi H, Gu Y, Xiu Y, Li B, Zhu W, et al. Differential diagnostic value of single-photon emission computed tomography/spiral computed tomography with Tc-99m-methylene diphosphonate in patients with spinal lesions. Nucl Med Commun. 2011;32(12):1194–200. [PubMed: 21934544]
15. Helyar V, Mohan HK, Barwick T, Livieratos L, Gnanasegaran G, Clarke SE, et al. The added value of multislice SPECT/CT in patients with equivocal bony metastasis from carcinoma of the prostate. Eur J Nucl Med Mol Imaging. 2010;37(4):706–13. [PubMed: 20016889]
16. Eary JF, O'Sullivan F, Powitan Y, Chandhury KR, Vernon C, Bruckner JD, et al. Sarcoma tumor FDG uptake measured by PET and patient outcome: a retrospective analysis. Eur J Nucl Med Mol Imaging. 2002;29(9):1149–54. [PubMed: 12192559]
17. Schuetze SM, Rubin BP, Vernon C, Hawkins DS, Bruckner JD, Conrad EU 3rd, et al. Use of positron emission tomography in localized extremity soft tissue sarcoma treated with neoadjuvant chemotherapy. Cancer. 2005;103(2):339–48. [PubMed: 15578712]
18. Evilevitch V, Weber WA, Tap WD, Allen-Auerbach M, Chow K, Nelson SD, et al. Reduction of glucose metabolic activity is more accurate than change in size at predicting histopathologic response to neoadjuvant therapy in high-grade soft-tissue sarcomas. Clin Cancer Res. 2008;14(3):715–20. [PubMed: 18245531]
19. Benz MR, Czernin J, Allen-Auerbach MS, Tap WD, Dry SM, Elashoff D, et al. FDG-PET/CT imaging predicts histopathologic treatment responses after the initial cycle of neoadjuvant chemotherapy in high-grade soft-tissue sarcomas. Clin Cancer Res. 2009;15(8):2856–63. [PubMed: 19351756]
20. Govaerts CW, van Dijken BR, Stormezand GN, van der Weide HL, Wagemakers M, Enting RH, et al. (11)C-methyl-L-methionine PET measuring parameters for the diagnosis of tumour progression against radiation-induced changes in brain metastases. Br J Radiol. 2021;94(1125):20210275. [PubMed: 34233489]
21. Glaudemans AW, Enting RH, Heesters MA, Dierckx RA, van Rheenen RW, Walenkamp AM, et al. Value of 11C-methionine PET in imaging brain tumours and metastases. Eur J Nucl Med Mol Imaging. 2013;40(4):615–35. [PubMed: 23232505]

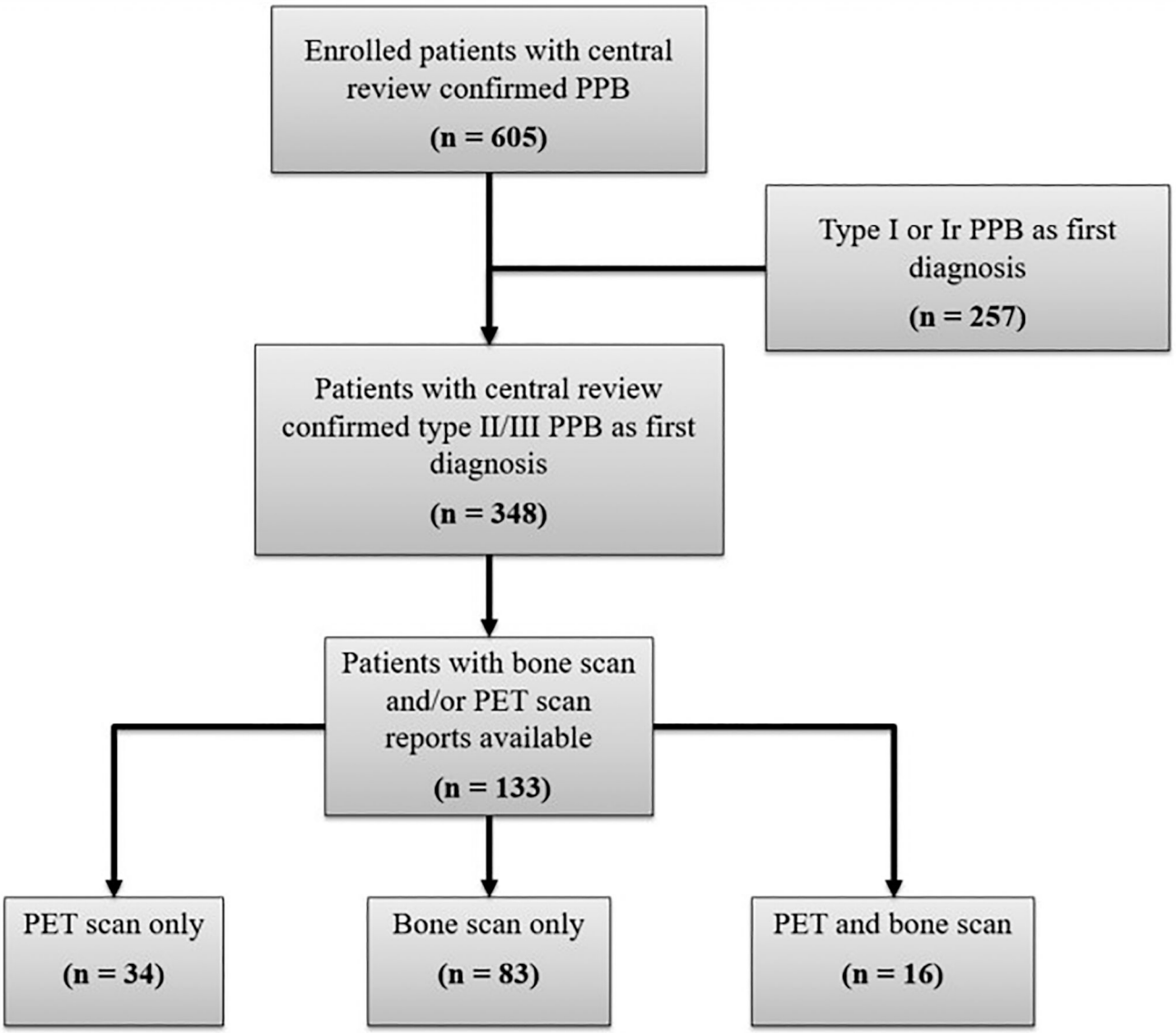

Fig 1.

Flow diagram of enrolled participants with centrally reviewed PPB and distribution of PET and bone scans among type II/III PPB.

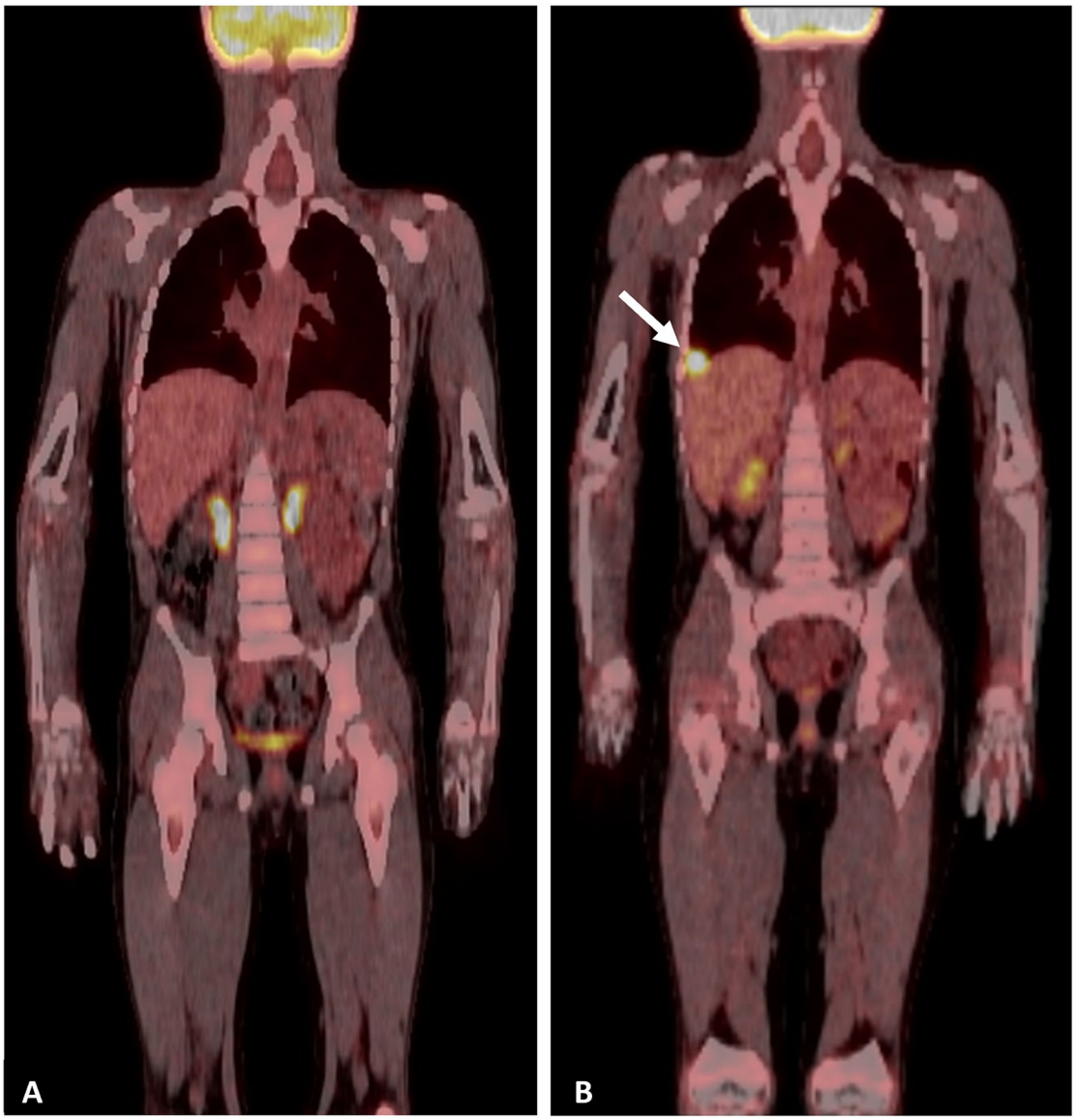

Fig 2.

Representative PET/CT scans **A**. Surveillance PET/CT after completion of treatment for type II PPB. **B.** Surveillance PET/CT showing detection of asymptomatic recurrent PPB in the right hemithorax (white arrow).

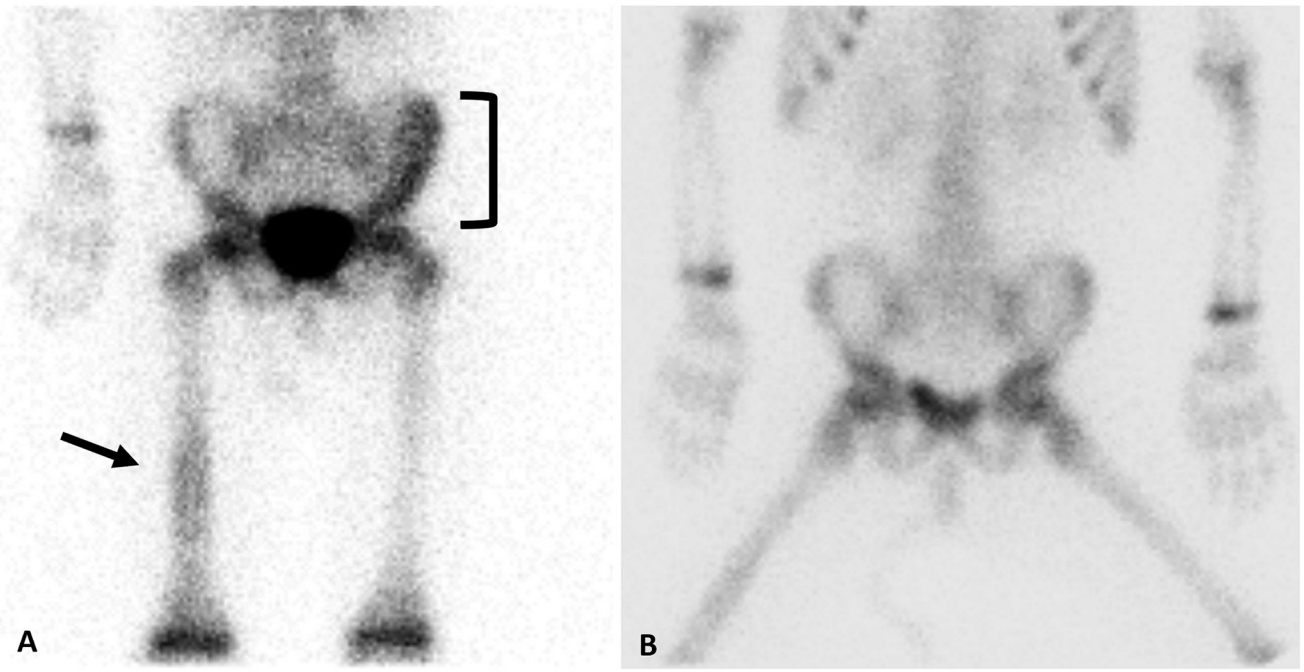

Fig 3.

Representative bone scans **A.** Bone scan prior to initial treatment of type III PPB representing abnormal radiotracer uptake involving the left ilium (black bracket) and right midshaft femur (black arrow). **B.** Bone scan during initial treatment demonstrating response to chemotherapy with osseous metastases appearing less conspicuous.

Table 1:

Classification of disease for PET and bone scan.

PET	
True positive	Primary tumors: if an FDG-avid lesion was confirmed as tumor at pathology. Metastatic lesions: if an FDG-avid lesion correlated with typical findings of metastasis via anatomic imaging or if the lesion was confirmed at pathology.
False positive	FDG-avid lesion on PET without evidence of disease on other imaging modalities or pathology, excluding postoperative changes.
True negative	Absence of FDG-avid lesion on PET with no findings of metastatic disease on other imaging modalities or pathology.
False negative	Absence of an FDG-avid lesion on PET with evidence of disease on other imaging modalities.
Bone scan	
True positive	Bone metastases on both bone scan and other imaging modalities with or without pathologic confirmation.
False positive	Abnormal uptake on bone scan without correlative features on other imaging modalities or with negative pathology.
True negative	No findings of metastatic disease on bone scan or other imaging modalities.
False negative	No findings of metastatic disease on bone scan with evidence of bone metastasis on other imaging modalities or pathology.

Table 2:

Characteristics of patients with PET only, bone scan only and both PET and bone scan.

	PET only (n=34)	Bone Scan only (n=83)	PET and Bone Scan (n=16)	Overall (n=133)
Sex				
Female, n (%)	20 (59)	46 (55)	9 (56)	75 (56)
Male, n (%)	14 (41)	37 (45)	7 (44)	58 (44)
Age at Diagnosis (m), median (r)	38 (3 – 235)	35 (5 – 222)	46 (22 – 183)	36 (3 – 235)
Year of Diagnosis, median (r)	2017 (2003 – 2022)	2007 (1983 – 2020)	2010 (2000 – 2020)	2010 (1983 – 2022)
Country of Origin				
USA, n (%)	28 (82)	73 (88)	15 (94)	116 (87)
Other, n (%)	6 (18)[a]	10 (12)[b]	1 (6)[c]	17 (13)
Initial PPB Diagnosis				
Type II, n (%)	21 (62)	54 (65)	5 (31)	80 (60)
Type III, n (%)	13 (38)	29 (35)	11 (69)	53 (40)
Number of Scans per Patient				
PET, median (range) [total]	2 (1 – 9) [79]	-	1 (1 – 10) [39]	2 (1 – 10) [118]
Bone Scan, median (range) [total]	-	1 (1 – 16) [208]	1 (1 – 3) [25]	1 (1 – 16) [233]
Relapsed Disease, n (%)	11 (32)	33 (40)	8 (50)	52 (39)
Deceased, n (%)	7 (21)	24 (29)	7 (44)	38 (29)

m = months, n = number, PET = Positron Emission Tomography, PPB – Pleuropulmonary blastoma, r = range

[a]- Canada (3), Spain (1), Saudi Arabia (1), Russia (1)

[b]- Canada (3), Australia (1), United Kingdom (1), Ireland (1), Bahrain (1), Hong Kong (1), Singapore (1), Saudi Arabia (1)

[c]- Czech Republic (1)

Table 3:

Relative SUV_{max} values for respective clinical contexts and PET-bone scan concordance.

Timing	N	FDG-Avid Lesion Reported n/N (%)	Max SUV FDG-PET Values, median [r]	PET-Bone Scan Concordance
Primary Site – Pre-Chemotherapy				
Diagnosis	11	11/11 (100)	7.4 [2.0–16.2] (n=9)[a]	NA
Resection with macroscopic residual disease	4	4/4 (100)	4.6 [3.3–7.0] (n=4)	NA
Resection with no residual disease	6	4/6 (67)	2.2 [1.5–2.8] (n=2)[a]	NA
Primary Site – Post-Adjuvant Chemotherapy				
Chest Recurrence Pre-Treatment	8	8/8 (100)	6.1 [1.6–12.7] (n=8)	NA
Surveillance	16	5/16 (31)	3 [1.3–5.3] (n=5)	NA
Metastatic Disease – Pre-Chemotherapy				
Distant Bone Metastasis at Diagnosis	3	3/3 (100)	2.5 [2.0–3.8] (n=3)	100% (3/3)
Distant Bone Metastasis at Relapse	2	2/2 (100)	3.2 [2.9–3.4] (n=2)	100% (1/1)
CNS Metastasis	3	0/3 (0)	NA	NA

CNS = central nervous system, FDG-PET = fluorodeoxyglucose-positron emission tomography, GTR = gross total resection, n = number, N = number assessed, r = range, SUV = standardized uptake value

[a] – Two patients without SUV_{max} value reported